Thermal Decomposition of ClOOCl†

R. Bröske and F. Zabel*,§

Bergische Universität Wuppertal, Physikalische Chemie/FB C, D-42097 Wuppertal, Germany

Received: September 5, 2005; In Final Form: December 20, 2005

ClOOCl was prepared in situ in a temperature controlled photoreactor ($v = 420$ L) by photolyzing $OClO/N_2$ mixtures in the wavelength range 300−500 nm at temperatures between 242 and 261 K and total pressures between 2 and 480 mbar. After switching off the lights, excess NO_2 was added, and IR and UV spectra were monitored simultaneously as a function of time. By spectral stripping of all other known UV absorbers (in particular, other chlorine oxides and chlorine nitrate), we determined rate constants k_{-1} of the reaction ClOOCl (+M) ⇒ ClO + ClO (+M) from the first-order decay of the residual UV absorption of ClOOCl at 246 and 255 nm. $k_{-1,0} = [N_2] \times 7.6 \times 10^{-9} \exp[(-53.6 \pm 6.0)\ \text{kJ mol}^{-1}/RT]\ \text{cm}^3\ \text{molecule}^{-1}\ \text{s}^{-1}$ (2σ) was derived for the low-pressure limiting rate constant. Application of Troe's expression for the limiting low-pressure rate constants of unimolecular decomposition reactions leads to $E_0 = \Delta_r H^0_0(\text{ClOOCl} \Rightarrow \text{ClO} + \text{ClO}) = 66.4 \pm 3.0\ \text{kJ mol}^{-1}$. $k_{-1,0}$ started to fall off from the pressure proportional low pressure behavior at $p \approx 30$ mbar; however, reliable extrapolation to the high pressure limit was not possible. The decomposition rate constants of ClOOCl were directly measured for the first time, and they are higher, depending on temperature and pressure, by factors between 1.5 and 4.2 as compared to experimental data on k_{-1} by Nickolaisen et al. [*J. Phys. Chem.* **1994**, *98*, 155] which were derived from the approach of ClO to thermal equilibrium with its dimer ClOOCl. Combination of the present dissociation rate constants with recommended temperature and pressure dependent data on the reverse reaction (k_1) demonstrate inconsistencies between the dissociation and recombination rate constants. Summarizing laboratory data on k_1 and k_{-1} above 250 K and field measurements on the ClO + ClO ⇔ ClOOCl equilibrium in the nighttime polar stratosphere close to 200 K, the expression $K_c = k_1/k_{-1} = 3.0 \times 10^{-27} \exp(8433\ \text{K}/T)\ \text{cm}^3\ \text{molecule}^{-1}$ is derived for the temperature range 200−300 K.

Introduction

The formation of ClOOCl by recombination of ClO in the cold polar stratosphere is, in addition to the presence of polar stratospheric clouds, a prerequisite for the formation of the Antarctic "ozone hole". ClOOCl is the key intermediate of an ozone destroying catalytic cycle:[1−3]

$$\text{ClO} + \text{ClO}\ (+\text{M}) \rightrightarrows \text{ClOOCl}\ (+\text{M}) \qquad (1)$$

$$\text{ClOOCl} + h\nu \rightrightarrows 2\text{Cl} + \text{O}_2 \qquad (2)$$

$$2\text{Cl} + 2\text{O}_3 \rightrightarrows 2\text{ClO} + 2\text{O}_2 \qquad (3)$$

$$\text{net:} \quad 2\text{O}_3 \rightrightarrows 3\text{O}_2$$

To a lesser extent, this catalytic cycle also takes place in the Arctic stratosphere,[4] and recently ClO and ClOOCl were simultaneously measured in the polar nighttime stratosphere for the first time.[5] In the polar spring, ClOOCl is rapidly photolyzed during the day, and the ClO concentration is then controlled by ClOOCl photolysis and ClO + ClO recombination. At and after sunset, ClO recombines to form ClOOCl. Because the thermal lifetime of ClOOCl is on the order of hours at the temperatures and pressures of the polar stratosphere,[6] the ClO concentration approaches thermal equilibrium with ClOOCl during the night. Thus, the actual concentrations of ClO and ClOOCl at sunset, during the night and in the early morning are also controlled by thermal decomposition of ClOOCl,

$$\text{ClOOCl}\ (+\text{M}) \rightrightarrows \text{ClO} + \text{ClO}\ (+\text{M}) \qquad (-1)$$

Because the nighttime concentrations of ClO in the Arctic stratosphere are at measurable levels (typically a few tens of ppt),[5,7−10] ClO concentrations (and, newly, also ClOOCl concentrations[5,10]) measured in the polar stratosphere can be used to test laboratory data on the kinetics of ClOOCl formation and decomposition. Most of the recent field measurements of ClO and ClOOCl were in general agreement with modeled concentrations based on laboratory data. However, discrepancies between measured and modeled ClO concentrations were also reported for both daylight[11,12] and nighttime measurements. In particular, several of the recent nighttime studies[5,7,10,12,13] favor values of the equilibrium constants k_1/k_{-1} that are lower than the currently recommended values[6] (see also the discussion by Plenge et al.[14]).

In the laboratory, the rate of reaction 1 has been extensively studied in the past in experimental[15−22] and theoretical[23] work, and a consistent data set[6] has been achieved from the data of several studies[19,20,22] over a wide range of temperatures and pressures. These data are thoroughly discussed in reviews and data compilations.[6,24,25] Thermal decomposition rate constants of ClOOCl (k_{-1}) have been deduced from the approach to thermal equilibrium of reaction systems that contain an excess

† Part of the special issue "Jürgen Troe Festschrift".

§ Present address: Institut für Physikalische Chemie der Universität, Universität Stuttgart, Pfaffenwaldring 55, D-70569 Stuttgart.

10.1021/jp0550053 CCC: $33.50
Published on Web 02/04/2006

of ClO,[20,21] and the equilibrium ClOOCl ⇔ ClO + ClO was studied in the temperature range 233−303 K.[26] The equilibrium (1,−1), however, may be affected by other channels of the ClO + ClO reaction[20,27,28] (see also refs 6, 24, and 25):

$$ClO + ClO \rightarrow Cl_2 + O_2 \quad (4a)$$

$$ClO + ClO \rightarrow Cl + ClOO \ (\rightarrow Cl + O_2) \quad (4b)$$

$$ClO + ClO \rightarrow Cl + OClO \quad (4c)$$

Because the data on k_1, k_{-1}, and k_1/k_{-1} are only in fair agreement and the majority of field measurements on the equilibrium between ClOOCl and ClO suggest lower than hitherto recommended equilibrium constants, a study of the thermal decay of ClOOCl seems to be desirable.

In the present work, k_{-1} is determined more directly than in previous experiments from the thermal first-order decay rate of ClOOCl in the temperature range 242−261 K at total pressures between 2 and 480 mbar,[29] allowing us to determine equilibrium constants by combining independently measured dissociation rate constants from this work and recombination rate constants from the literature.

Experimental Section

ClOOCl was prepared in situ in a 420 L temperature controlled photoreactor from DURAN glass equipped with Teflon-coated end flanges from aluminum by photolyzing OClO/N_2 mixtures at 300 nm ≤ λ ≤ 500 nm with 20 fluorescent lamps (Philips TLA 40W/05). The reaction chamber is described in more detail by Barnes et al.[30] The kinetic behavior of the OClO photolysis system under the present reaction conditions is quite complex and was elucidated in previous work.[31] Because interfering UV absorptions from other species (ClO, OClO, $ClClO_2$, Cl_2O_3, Cl_2O_4, Cl_2, NO_2, $ClONO_2$) were involved, simultaneous qualitative and quantitative characterization of these species by their IR and UV absorption spectra proved to be essential.

At total pressures of several mbar, the main feature of the OClO photolysis reaction system is the photolysis of OClO,

$$OClO + h\nu \rightarrow ClO + O \quad (5)$$

followed by the reactions

$$ClO + ClO\ (+M) \leftrightarrow ClOOCl\ (+M) \quad (1,-1)$$

$$ClO + OClO\ (+M) \leftrightarrow Cl_2O_3\ (+M) \quad (6,-6)$$

$$Cl + OClO\ (+M) \rightarrow ClClO_2\ (+M)\ (?) \quad (7)$$

$$Cl + ClOOCl \rightarrow Cl_2 + Cl + O_2 \quad (8)$$

$$Cl + ClClO_2 \rightarrow Cl_2 + OClO \quad (9)$$

$$O + OClO \rightarrow O_2 + ClO \quad (10)$$

Finally, the photolysis mixture contains molecular chlorine and the chlorine oxides ClOOCl, ClO, OClO, $ClClO_2$, and Cl_2O_3. Microwave studies have shown that the recombination product of the ClO self-reaction is dichlorine peroxide[32] although ab initio calculations do suggest that other isomers (ClOClO, $ClClO_2$) also exist.[23,33−35] In fact, $ClClO_2$ has been synthesized and identified by Müller and Willner.[36] The mechanism of $ClClO_2$ formation in the present reaction system is yet unknown. However, heterogeneous formation of $ClClO_2$ in the presence of water ice is discussed in the literature.[37,38] The increase of relative $ClClO_2$ yields with decreasing total pressure observed in our reaction system suggests that wall reactions are involved in its formation.

After the concentration of ClOOCl has reached its maximum, the lights are switched off and an excess of NO_2 is added to the reaction mixture. The main effect of NO_2 is to scavenge ClO radicals very rapidly by reaction 11,

$$ClO + NO_2\ (+M) \rightarrow ClONO_2\ (+M) \quad (11)$$

and thus to prevent ClO radicals from forming ClOOCl and Cl_2O_3 back via reactions 1 and 6. Cl_2O_3 (fast) and ClOOCl (slow) then disappear according to first-order processes whereas $ClONO_2$ is thermally stable under the reaction conditions of this work.[39]

At total pressures above 30 mbar, the yield of ClOOCl in the photolysis of OClO was too low for the decay rate in the dark to be measured. Under these conditions, Cl_2O_4 is the predominant chlorine oxide formed, probably due to the increase of the recombination rate of O and OClO with total pressure, leading to Cl_2O_4 via the short-lived intermediate ClO_3.[31] In experiments at these "high pressure" conditions, ClOOCl was first generated by photolysis of OClO at a reduced pressure of 2 mbar. In a second step, the buffer gas N_2 was added up to the desired total pressure before starting the decomposition experiment in the dark by adding NO_2.

UV absorption is measured using a concave mirror with single reflection (optical path length 3.1 m), a deuterium lamp (20 W) and a diode array spectrometer that consists of a monochromator (Spex 1680, f = 22 cm) modified to act as a spectrograph, and a diode array (EG&G Parc 1412). Spectral resolution is 0.3 nm, the photon collection time of a single scan was 1.0−1.5 s. IR spectra were monitored simultaneously to the UV spectra by long-path absorption (50.4 m), using a White mirror system and an FT-IR spectrometer (NICOLET Magna 550, HgCdTe detector, spectral resolution 1 cm^{-1}).

The reaction temperature is measured using a platinum resistance gauge that extends from the end flange into the reaction chamber by 20 cm. During an experiment, the temperature is constant within 0.5 K.

The chlorine oxides ClOOCl, Cl_2O_3, $ClClO_2$, and Cl_2O_4 were identified and quantitatively estimated using characteristic IR and UV absorption features. UV reference spectra of $ClClO_2$ were obtained from reaction mixtures containing very different concentration ratios of ClOOCl and $ClClO_2$. A reference spectrum of $ClONO_2$ was obtained from the photolysis of a 1:1 mixture of OClO and NO_2, using N_2 as a buffer gas. The reaction mechanism was modeled for both the photolysis and the dark period, using the program LARKIN by Deuflhard and Nowak.[40] Initial concentrations of OClO were between 1.1 × 10^{15} and 2.0 × 10^{15} molecule cm^{-3}. N_2 was used as a buffer gas. The OClO conversion was between 90% and 20%, depending on temperature. ClOOCl concentrations at the beginning of the dark period were (2.5−11.5) × 10^{13} molecule cm^{-3}. The added amounts of NO_2 correspond to (2−8) × 10^{14} molecule cm^{-3}, part of which was consumed immediately by scavenging the free ClO radicals. In total, about 7−32% of the added NO_2 was consumed during the experiment. Photolysis times were 100−600 s; observation times in the dark were between 10 s and 30 min, depending on temperature and pressure.

OClO was prepared from $KClO_3$ and sulfuric acid in the presence of oxalic acid.[41]

TABLE 1: UV and IR Absorption Cross Sections σ Used To Estimate Species Concentrations ($\sigma = \ln(I_0/I)/(cd)$)

molecule	ω_{IR} [cm^{-1}]	λ_{UV} [nm]	$10^{18}\sigma$ [cm^2 $molecule^{-1}$]	ref
OClO	2049		~0.014	31
ClOOCl		246	6.49	42
	653		0.036	43
$ClClO_2$		240	10.6	36
Cl_2O_4		245	0.72	44
	1282		~2.3	31
$ClONO_2$		255	0.391	45
$ClNO_2$	1267		0.48	46
		240	1.40	47
HNO_3	878		0.71	46
		238	0.0293	48

Results

IR band positions as well as IR and UV absorption cross sections used for identification and quantification of the educts and products are collected in Table 1. In Figure 1, IR spectra are shown for the same experiment (a) directly after switching off the photolysis lamps, (b) 90 s after the addition of NO_2, and (c) at the end of the experiment, i.e., after ClOOCl has been consumed. The main features of the IR product spectra in Figure 1a − 1c at different reaction times are described in the following.

(a) Figure 1a shows residual absorption from OClO (1100 cm^{-1}) and product absorptions from ClOOCl (653 cm^{-1}), Cl_2O_3 (740, 1058, 1224 cm^{-1}), and Cl_2O_4 (659, 1285 cm^{-1} [49]). Because the intensity ratio of the Cl_2O_4 bands at 659 and 1285 cm^{-1} is about 0.5,[31] Figure 1a shows that the absorption at 653 cm^{-1} mainly originates from ClOOCl. The IR absorption at this wavenumber, however, is not appropriate to measure the decay rate of ClOOCl due to both its low intensity (σ(653 cm^{-1}) = 3.6×10^{-20} cm^2 $molecule^{-1}$ [43]) and its interference with Cl_2O_4. Comparing the absorption bands centered at 1042 and 1218 cm^{-1} with the spectrum from Müller and Willner[36] of a pure sample of $ClClO_2$ shows that $ClClO_2$ is also formed in our reaction system.

(b) The IR spectrum in Figure 1b is dominated by absorption from $ClONO_2$ (780, 809, 1293, 1737 cm^{-1} [50]) and excess NO_2 (around 1600 cm^{-1}). Absorption from Cl_2O_3 has already disappeared.

(c) $ClONO_2$ has further increased, residual OClO and NO_2 are present, Cl_2O_2 and $ClClO_2$ have disappeared. Closer inspection of the IR spectra at late reaction times shows that small absorptions from $ClNO_2$, HNO_3, and $HClO_4$ (probably from wall reaction of Cl_2O_4[31]) are also present. However, the UV absorptions from these species are negligible.

After the addition of NO_2, the loss of Cl_2O_3 is faster by more than a factor of 10 than the decay of ClOOCl (as estimated from the ClO + OClO recombination rate constant k_6[6,51,52] and the equilibrium constant k_6/k_{-6}[6,53,52]). Cl_2O_3 thus disappears immediately after the addition of NO_2, as is evidenced by the product spectra in both the IR and UV regions. The decay rate of $ClClO_2$ is comparable to that of ClOOCl; thus, correction of the product UV spectrum for the absorption from $ClClO_2$ is essential. At higher total pressures, Cl_2O_4 is also formed, which is thermally stable under the present reaction conditions.[31,44] $ClONO_2$ is continuously formed during the reaction and adds to the total UV absorption at the wavelengths used for the analysis of ClOOCl.

Due to their much stronger absorption cross sections in the UV as compared to the IR region, the concentration−time behavior of ClOOCl has been followed in the UV region, although a thorough and extensive data treatment of the UV spectra was necessary to allow for several interfering UV absorbers: OClO, $ClClO_2$, Cl_2O_4, $ClONO_2$, and NO_2. The much better signal-to-noise ratio for the UV absorptions of ClOOCl also allowed a better time resolution on the order of 1 s.

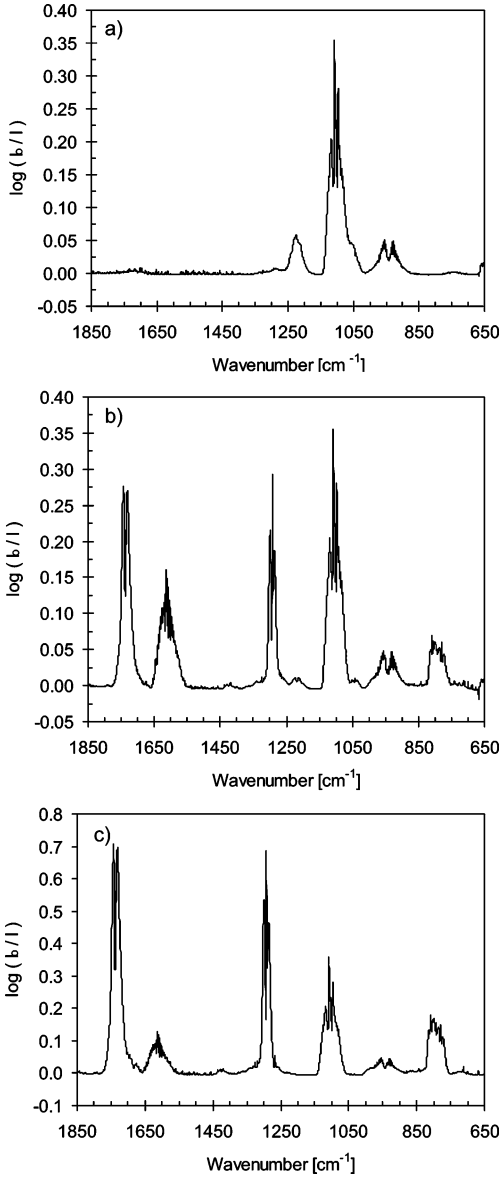

Figure 1. IR spectra of a photolyzed $OClO/N_2$ mixture after termination of photolysis; T = 258.7 K, p_{tot} = 2.1 mbar; $[OClO]_0 = 1.4 \times 10^{15}$ molecule cm^{-3}; photolysis time, 200 s. Key: (a) directly after switching off the photolysis lights; (b) 80 s after the addition of NO_2; (c) 5 min after the addition of NO_2.

A series of consecutive UV product spectra after switching off the photolysis lamps are shown in Figure 2 for the same experiment as in Figure 1. The reaction time increases from top to bottom. Consecutive spectra are taken every 15 s. NO_2 was addded after the third spectrum from the top. The strong decrease of absorption between 260 and 280 nm from the third to the fifth spectrum indicates the rapid decay of Cl_2O_3. In addition, the weak structured absorption from ClO in the vicinity of 270 nm disappears after the addition of NO_2. At long reaction times, the spectra approach a spectrum that is dominated by $ClONO_2$ and residual absorption from NO_2 (near 242 nm) and OClO (>260 nm).

A single product UV spectrum, e.g., one of the spectra in Figure 2, was treated the following way: the presence of potential UV absorbers was verified by the simultaneously

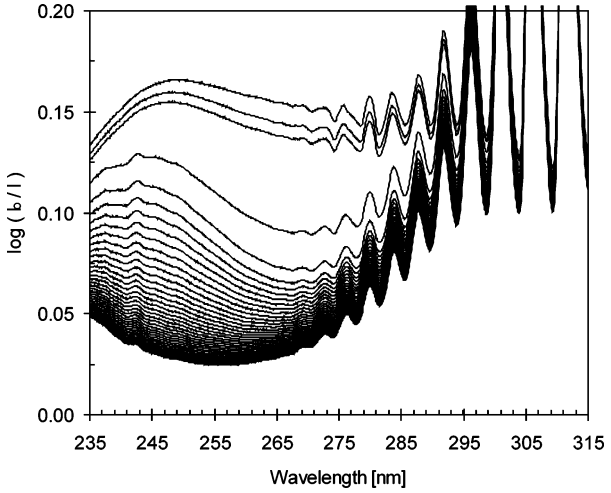

Figure 2. UV spectra of a photolyzed mixture of OClO and N_2 after termination of photolysis (same experiment as in Figure 1, consecutive spectra (every 15 s) from top to bottom); $[NO_2]_0 = 3.9 \times 10^{14}$ molecule cm^{-3}, added between third and fourth spectrum.

measured IR absorption bands. The contribution of an individual absorber to the product UV spectrum was then quantified by the relative IR absorptions in the product spectrum and a calibration spectrum, using the relationship:

$$\text{UV absorbance(experiment)} = \text{UV absorbance (calibration)} \times [\text{IR absorption(experiment)/IR absorption (calibration)}]$$

The calibration spectra were obtained from pure compounds (for OClO, NO_2) and from product spectra of particular reaction mixtures generated at reaction conditions which favor the formation of individual species (for Cl_2O_2, $ClClO_2$, Cl_2O_4, $ClONO_2$). Where available, IR absorption coefficients from the literature were used for a rough estimate of the species concentrations. In several cases, UV absorption cross sections from the literature were used to determine IR absorption coefficients.

In detail, the spectral stripping procedure includes

(i) subtraction of NO_2 via its structured absorption close to 242 nm;

(ii) subtraction of OClO via its banded structure below 285 nm; the absorption above 285 nm did not obey Beer's law (the initial OClO spectrum was used as a reference for the individual experiments);

(iii) subtraction of $ClONO_2$ and $ClClO_2$ according to their IR absorptions at 809 and 1224 cm^{-1}, respectively, based on the IR and UV absorbance ratios in simultaneously measured reference spectra; and

(iv) in several experiments, subtraction of Cl_2 based on a rough Cl balance that was inaccurate mainly due to the strong absorption from OClO, which did not obey Beer's law (below 260 nm, however, absorption from Cl_2 was negligible).

The result of this spectral stripping procedure is depicted in Figure 3 for the same experiment as in Figures 1 and 2. Between 240 and 290 nm, the relative absorptions at different wavelengths in the residuals of this stripping procedure agree with the UV absorption cross sections of ClOOCl from Burkholder et al.[42] (see Figure 3). Typical initial concentrations derived in this manner for the early stages of the decomposition reaction were as follows (in units of 10^{13} molecule cm^{-3}): 5.5 (ClOOCl), 43 (NO_2), 110 (OClO), 17 ($ClONO_2$), 0.90 ($ClClO_2$), 33 (Cl_2). Figure 4 shows the residuals which are obtained when in Figure 3 the uppermost spectrum is subtracted from the subsequent

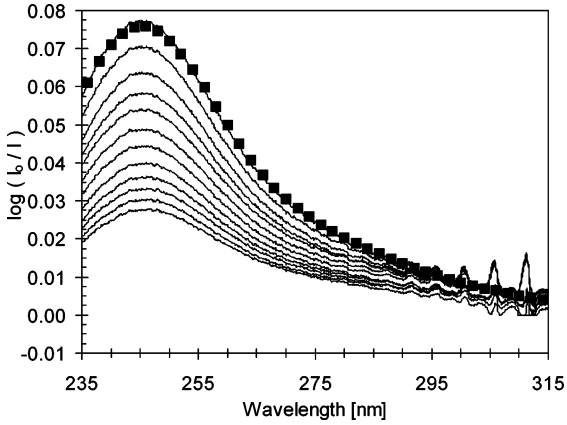

Figure 3. Product UV absorptions from ClOOCl as a function of time in a photolysis mixture of $OClO/N_2$ after termination of photolysis and addition of excess NO_2 (same experiment as in Figures 1 and 2); $T = 258.7$ K, $p_{tot} = 2.1$ mbar; $[OClO]_0 = 1.4 \times 10^{15}$ molecule cm^{-3}; photolysis time, 200 s. Consecutive spectra (from top to bottom, every 15 s) are derived from spectra no. 6−17 (from top to bottom) in Figure 2. Key: full squares, fit of the absorption coefficients of ClOOCl from Burkholder et al.[42] to the uppermost absorption trace with [ClOOCl] $= 8.7 \times 10^{13}$ molecule cm^{-3}.

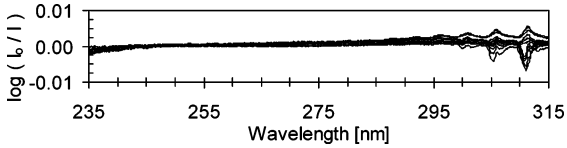

Figure 4. Residuals obtained by subtracting the uppermost spectrum in Figure 3 (assigned to ClOOCl) from the subsequent spectra using appropriate calibration factors, demonstrating that the shape of the ClOOCl spectra does not change significantly with time (same scale as in Figure 3).

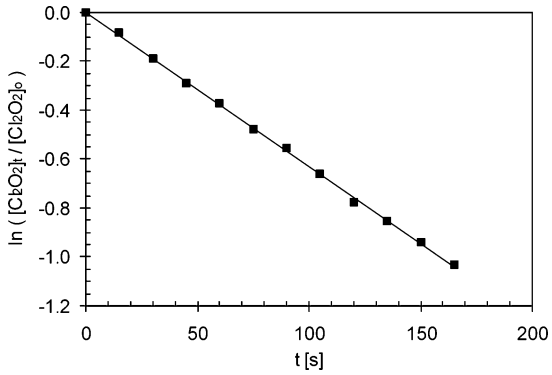

Figure 5. Concentration−time profile for thermal decomposition of ClOOCl. Reaction conditions (same experiment as in Figures 1−3): $T = 258.7$ K, $p_{tot} = 2.1$ mbar; $[OClO]_0 = 1.4 \times 10^{15}$ molecule cm^{-3}. Key: full squares, based on the average of the absorbances at 246 and 255 nm of the residual spectra shown in Figure 3; $k_{-1} = 6.16 \times 10^{-3}$ s^{-1}.

spectra using appropriate calibration factors. Figure 4 demonstrates that the shape of the ClOOCl spectra does not change significantly with time, in particular at the wavelengths used for the evaluation of k_{-1} (i.e., at 246 and 255 nm, see below). In Figure 5, a logarithmic plot of the relative ClOOCl concentrations as a function of time is shown for the absorption spectra in Figure 3, based on the average of the absorbances at 246 nm (absorption maximum) and 255 nm.

The decay rate of $ClClO_2$ was comparable to that of ClOOCl at low temperatures and pressures but considerably slower at higher temperatures and pressures. In several additional experiments it was shown that in a mixture of ClOOCl and $ClClO_2$,

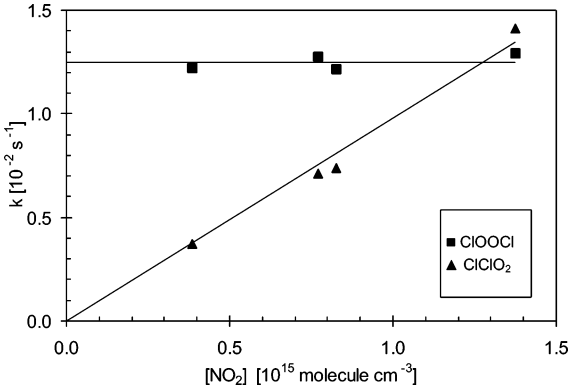

Figure 6. First-order decay rate constants of [ClOOCl] and [$ClClO_2$] in the presence of different concentrations of excess NO_2; $T = 258.45 \pm 0.25$ K; $p_{tot} = 4.0$ mbar, M = N_2.

after the addition of different amounts of NO_2, the decay of ClOOCl was independent of the NO_2 concentration. In contrast to this, $ClClO_2$ decayed with a first-order rate constant that was proportional to the NO_2 concentration (Figure 6). At the same time, the formation of $ClNO_2$ was observed via its IR spectrum. This behavior suggests that, in the presence of NO_2, $ClClO_2$ undergoes a rapid bimolecular reaction with NO_2 forming $ClNO_2$ whereas ClOOCl decays by thermal decomposition. No efforts were made to determine unimolecular decomposition rate constants of $ClClO_2$ because the contributions of bimolecular reactions and/or wall loss were unknown.

Mass balances for chlorine were made only in a few runs because the derivation of the Cl_2 concentration from its UV absorption was too inaccurate due to the strong overlap of the UV absorptions of Cl_2 and OClO. The UV spectra of ClOOCl obtained after spectral stripping of NO_2, ClO, OClO, $ClClO_2$, Cl_2O_4, and $ClONO_2$ (see Figure 3) were evaluated according to a first-order rate law. Due to the laborious stripping procedure, only part of the product spectra from each experiment were evaluated (e.g., in Figure 2: spectra no. 6−17 from top to bottom). The resulting first-order decomposition rate constants are summarized in Table 2.

It is worth noting that the original UV spectra (for example those in Figure 2) could also be evaluated according to a first-order rate law, based on plots of ln(absorbance at 255 nm at time t minus absorbance at 255 nm for $t \Rightarrow \infty$) as a function of time for all absorbance traces of a single experiment after the addition of NO_2 (i.e., for 36 data points in the experiment shown in Figure 2). This first-order behavior is to be expected if educt and product absorptions change according to the same order and with the same time constant. This was obviously true for the absorbance at 255 nm which was used to estimate k_{-1} by this method. The rate constants determined by both methods were identical within error limits. All of the rate constants in Table 2, however, were derived from the ClOOCl absorption spectra (e.g., those in Figure 3) obtained after the spectral stripping procedure.

The first-order decomposition rate constants summarized in Table 2 depend on temperature and total pressure. Arrhenius plots of the rate constants obtained at 4, 8, 16, 32, 64, and 128 mbar are shown in Figure 7. These data points were derived from measurements in small pressure ranges around the stated pressure by correcting for the small difference in pressure, based on the relationship $k_{-1} \propto [M]^x$ with $x = 1$ for the experiments below 30 mbar (limiting low-pressure range) and $x = 0.8-0.95$ at higher pressures (falloff range).

In Figure 8, the data are displayed as falloff curves, showing that the rate constants are close to the low-pressure limit. The

TABLE 2: Summary of Experimental Results on k_{-1}

244 ± 2 K			248 ± 2 K		
T [K]	10^{-18}[M] [molecule cm^{-3}]	$10^3 k_{-1}$ [s^{-1}]	T [K]	10^{-18}[M] [molecule cm^{-3}]	$10^3 k_{-1}$ [s^{-1}]
242.65	0.115	2.30	247.63	0.117	4.67
244.15	0.252	5.10	247.65	0.123	4.08
244.95	0.256	5.70	247.68	0.244	6.96
243.65	0.522	8.55	247.85	0.447	11.55
244.15	0.546	9.25	248.25	0.880	20.20
243.15	1.030	15.10	248.40	0.894	21.25
244.15	1.060	16.65	248.80	1.810	38.27
246.15	1.950	32.30	248.40	1.770	31.39
245.35	2.000	29.60	249.40	3.620	82.90
246.75	3.720	51.35	250.15	3.630	74.91
246.25	3.730	48.55	248.15	7.340	84.50
			248.15	7.330	102.75
			247.00	14.00	139.00
			247.45	13.90	147.00
			247.25	14.10	148.00
254 ± 2 K			259 ± 2 K		
T [K]	10^{-18}[M] [molecule cm^{-3}]	$10^3 k_{-1}$ [s^{-1}]	T [K]	10^{-18}[M] [molecule cm^{-3}]	$10^3 k_{-1}$ [s^{-1}]
252.90	0.0619	3.87	260.80	0.0564	7.50
254.50	0.0620	3.88	258.70	0.0580	6.16
255.40	0.0624	4.54	258.60	0.113	12.23
251.80	0.0636	3.54	258.70	0.113	12.13
252.00	0.0713	4.20	258.20	0.114	12.94
251.80	0.120	6.82	258.70	0.114	11.90
252.00	0.121	6.30	258.60	0.114	12.78
252.30	0.122	7.62	258.95	0.225	22.40
256.20	0.122	8.67	258.40	0.446	40.80
252.00	0.232	10.90	257.95	0.489	44.40
254.90	0.231	10.80	258.35	0.530	46.50
254.30	0.459	23.94	258.20	0.874	71.50
254.00	0.876	34.30	258.65	0.878	63.10
254.50	0.920	45.00	258.25	0.900	77.25
253.80	1.790	69.40	259.10	0.872	77.25
253.50	1.810	66.10			
254.45	3.590	123.30			
253.60	7.230	201.50			

pressure dependence of k_{-1} can be discussed in terms of the parametrization suggested by Troe.[54] To meet the format of the JPL data compilation,[6] the simplest version of the falloff equations was applied:

$$\log(k/k_\infty) = \log\{(k_0/k_\infty)/(1 + k_0/k_\infty)\} + \log(F_c)\{1 + [\log(k_0/k_\infty)]^2\}^{-1} \quad \text{(I)}$$

with $F_c = 0.6$ and $N_c = 1$ (thus disappearing in eq I), neglecting the temperature dependence of F_c due to the small temperature

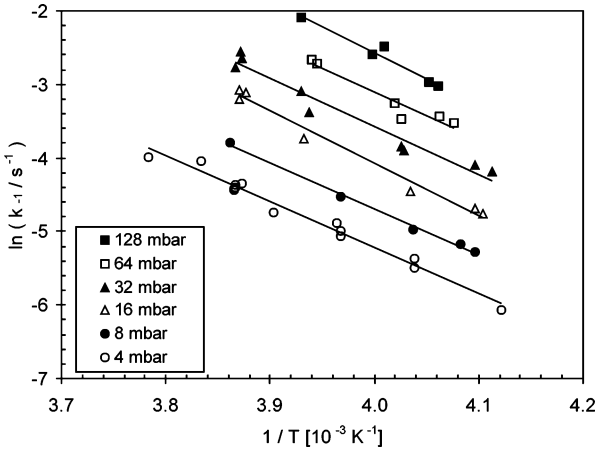

Figure 7. Arrhenius plots of k_{-1} at different total pressures (M = N_2).

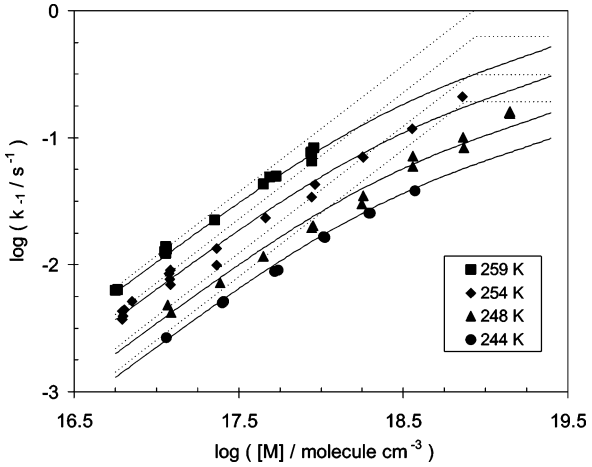

Figure 8. Falloff curves for k_{-1} at 259, 254, 248, and 244 K.

range investigated in this work. The falloff curves calculated from eq I were fitted to the data of Table 2 at four temperatures, i.e., 244, 248, 254, and 259 K. Each of the individual falloff curves yielded both a limiting low- and high-pressure rate constant. Because the data were close to the low-pressure limit, the resulting limiting first-order low-pressure rate constants k_0 are much more reliable than the high-pressure limiting rate constants k_∞. In a second step, the falloff curves obtained at different temperatures were adjusted to the experimental data such that both the k_0 and k_∞ values obey Arrhenius laws. The resulting pressure dependencies are shown in Figure 8; they are represented by eq I with the parameters

$$k_0(T) = [\mathrm{N_2}] \times 7.6 \times 10^{-9} \exp[-53.6\ \mathrm{kJ\ mol^{-1}}/RT]\ \mathrm{cm^3\ molecule^{-1}\ s^{-1}}$$

$$k_\infty(T) = 2.0 \times 10^{12} \exp[-60.8\ \mathrm{kJ\ mol^{-1}}/RT]\ \mathrm{s^{-1}}$$

$$F_c = 0.6$$

Figure 8 shows that the measured rate constants are close to the low-pressure limit under most of the reaction conditions but a deviation from the low-pressure limit is discernible at the highest pressures applied. However, reliable extrapolation to the high pressure limit was not possible. In Figure 8, data points at a stated temperature T were obtained by converting rate constants measured in a temperature range $T \pm 2$ K to the stated temperatures using an estimated Arrhenius energy. Due to the small temperature ranges of ± 2 K, errors of k_{-1} introduced by this procedure were negligible.

Discussion

A. Mechanism. The observed loss of ClOOCl in the dark was assigned to unimolecular gas-phase decomposition. Other possible loss processes are wall loss, reaction with Cl atoms, and reaction with NO_2. Estimates based on (i) the photolysis rate of Cl_2, (ii) the rate constants of the reactions of Cl atoms with ClOOCl,[26] OClO,[6] and NO_2,[6] and (iii) typical concentrations of these possible reactants show that the reaction of Cl atoms with OClO is faster by an order of magnitude as compared to the reaction with ClOOCl. In particular, however, it is difficult to see how Cl atoms can be formed in the dark. ClO radicals are able to form Cl atoms by self-reaction, reactions 4b and 4c; however, scavenging of ClO by NO_2 is very efficient under our conditions in the dark: even at the highest temperatures and pressures used in this work, the rate of the ClO self-reaction to form Cl atoms is only about 10^{-3} of the rate of the ClO + NO_2 recombination. Reaction of ClOOCl with NO_2 is unimportant, as was shown in the previous section (Figure 6). Wall loss should depend on the rate of diffusion to the walls and thus on total pressure. As a matter of fact, decay rate constants for ClOOCl measured at 1 mbar total pressure seem to be slightly faster than is suggested by a limiting low-pressure behavior and were discarded. These deviations from the low-pressure limit would be expected to accelerate at still lower pressures; however, reliable loss rates of ClOOCl could not be measured below about 0.5 mbar due to leak rates changing the total pressure and the collision partner composition during the experiment.

TABLE 3: Limiting Low Pressure Rate Constants $k_{-1,0}$/[M] for Decomposition of ClOOCl

ref	$k_{-1,0}$(250 K)/[M] [cm^3 molecule^{-1} s^{-1}]	M	T range [K], remarks
20	$1.3_5 \times 10^{-20}$	N_2	260−310
23	3.5×10^{-22}	N_2	ab initio calculation
this work	4.8×10^{-20}	N_2	242−261

Other unimolecular decomposition channels of ClOOCl are

$$\mathrm{ClOOCl\ (+M) \rightleftharpoons Cl + ClOO\ (+M)} \quad (12)$$

$$\mathrm{ClOOCl\ (+M) \rightleftharpoons Cl_2 + O_2\ (+M)} \quad (13)$$

$$\mathrm{ClOOCl\ (+M) \rightleftharpoons OClO + O\ (+M)} \quad (14)$$

The existence of channels (12)−(14) could be excluded by DeMore and Tschuikow-Roux.[55]

B. Temperature and Pressure Dependence of k_{-1}. The results of the present work may be compared with data on k_{-1} from the literature that were derived from the approach of the system ClO + ClO to equilibrium[20] and from an ab initio calculation[23] (Table 3).

The dissociation rate constants of ClOOCl from this work are higher than previous values from Nickolaisen et al.[20] by factors between 1.5 and 4.2, depending on temperature and total pressure. The reasons for these discrepancies are yet unknown. Nickolaisen et al. used flash photolysis of Cl_2O/Cl_2 mixtures as a source of ClO, and UV absorption to follow the decay of ClO radicals and the formation of the product OClO. Whereas the loss rate of ClO is dominated by self-reaction to form ClOOCl at $T < 250$ K, thermal decomposition of ClOOCl and the bimolecular reaction channels 4a, 4b, and 4c become increasingly important at $T > 250$ K. Reaction conditions were varied over a wide range of temperatures, pressures and initial concentrations of Cl_2 and Cl_2O to unravel these different processes. Measured temporal concentration profiles of ClO and OClO were fitted by model calculations using these rate constants as input parameters. Temperature-dependent rate constant expressions were presented for k_1, k_{-1}, k_{4a}, k_{4b}, and k_{4c}.

The reason for the difference between the results on k_{-1} from these two studies is yet unknown. In our study, it is difficult to definitely exclude enhancement of the decomposition rate by reaction on the walls of the reaction chamber. However, we believe that loss of ClOOCl on the walls is not important at our reaction conditions: decay rate constants would be expected to become increasingly important at lower pressures due to increasing transport to the chamber walls. In contrast, the measured first-order rate constants smoothly approach the low pressure limit with decreasing total pressure, and only at and below 1 mbar do small deviations become apparent (see above). Alternatively, the correct consideration of the bimolecular channels 4a−4c could pose problems to the determination of

TABLE 4: Values for Equilibrium Constants $K_c = k_1/k_{-1}$ at 200, 250, and 298 K and the Enthalpy of Reaction (−1)

ref	T (range) [K]	K_c(200 K) [cm^3 molecule^{-1}]	K_c(250 K) [cm^3 molecule^{-1}]	K_c(298 K)[a] [cm^3 molecule^{-1}]	$\Delta_r H^0_T$ [kJ mol^{-1}]
16	298			5.15×10^{-15}	69 ± 3[b]
26	233−303		1.44×10^{-12} [c]	6.24×10^{-15}	72.5 ± 3[d,e]
20	260−310		2.60×10^{-12} [f]	8.86×10^{-15}	76.6 ± 2.9[b,g]
27	285			6.16×10^{-15} [h]	
21	295			4.80×10^{-15} [i]	
6	200−300	12.3×10^{-9}	1.97×10^{-12} [j]	7.03×10^{-15} [j]	75.7 ± 2.9[b]
14			0.91×10^{-12} [k]	3.7×10^{-15} [k]	72.4 ± 2.8[b]
7	188−209	6.70×10^{-9} [l,m]			
10	192−216	1.96×10^{-9} [l,n]			
this work	243−261		0.85×10^{-13} [o]	4.7×10^{-15} [o]	69.4 ± 4.6[o,p]

[a] Extrapolation to 298 K with eq VII (see below). [b] At 298 K. [c] $K_{eq} = 2.5 \times 10^{-27}$ exp (8497 K/T) cm^3 molecule^{-1}. [d] We estimate a 2σ error of $\pm$ 4.6 kJ mol^{-1} from their K_p(T) data. [e] At a mean temperature of 263 K. [f] $K_{eq} = 1.24 \times 10^{-27}$ exp(8820 K/T) cm^3 molecule^{-1}. [g] From the heat of formation of ClOOCl at 298 K cited in ref 20 as their experimental result and the heat of formation of ClO in JPL 94. [h] Experimental value: K_{eq}(285 K) = $(2.24 \pm 0.35) \times 10^{-14}$ cm^3 molecule^{-1}. [i] Experimental value: $K_{eq} = (6.4 \pm 1.6) \times 10^{-15}$ cm^3 molecule^{-1} at 295 K. [j] From $K_{eq} = 1.27 \times 10^{-27}$ exp(8744 K/T) cm^3 molecule^{-1}. [k] The absolute K_{eq} values have large error limits because the uncertainty of $\Delta_r H^0_{298}$ directly translates into the uncertainty of K_{eq}. [l] Field measurement. [m] $K_{eq} = 1.99 \times 10^{-30} T$ exp(8854 K/T) cm^3 molecule^{-1} at a mean temperature of 198 K. [n] $K_{eq} = 3.61 \times 10^{-27}$ exp(8167 K/T) cm^3 molecule^{-1} at a mean temperature of 203 K. [o] From the "low pressure" data set; see text. [p] At a mean temperature of 252 K.

k_{-1} in the fitting procedure of Nickolaisen et al.[20] The branching ratios of reaction 4 are not yet well understood. For example, k_{4b}/k_{4a}(298 K) = 1.65 (ClO regenerating vs molecular product channel) was determined by Nickolaisen et al. whereas there is evidence from other laboratories that this ratio may be close to 1[27,56] at 298 K.

The low value for k_{-1} determined in the ab initio study[23] probably originates from an error in the calculated bond energy of the order of 10 kJ mol^{-1}.[57]

The low-pressure rate constant $k_{-1,0}$ measured in this work may be compared with the predictions of the low-pressure rate constant expression of Troe:[54,58]

$$k_0 = \beta_c[\mathrm{M}]Z_{LJ}\rho_{vib,harm}(E_0)(Q_{vib}{}^{-1}) \exp(-E_0/RT)RT\,F_E F_{anh} F_{rot} \quad \text{(II)}$$

with $\beta_c = k_{exp}/k_{calc}$, Z_{LJ} = Lennard-Jones collision number, E_0 = reaction barrier, $\rho_{vib,harm}(E_0)$ = density of states at $E = E_0$, Q_{vib} = vibrational partition function, F_E = correction for increased density of states at $E > E_0$, F_{anh} = correction for anharmonicity of fundamentals, F_{rot} = correction for rotational states. The measured low-pressure limiting rate constant at 250 K is used to estimate $E_0 = \Delta_r H^0_0$ from eq II by (i) setting $\beta_c = 0.3$, which is a typical value for M = N_2 at low temperatures,[59] (ii) using the vibrational wavenumbers 754,[60] 648,[60] 543,[60] 419,[60] 321,[35] and 127[32] cm^{-1} as discussed by Jacobs et al.,[60] and (iii) calculating Z_{LJ}(250K) = 3.6×10^{-10} cm^3 molecule^{-1} s^{-1} with molecular parameters of ClOOCl from Bloss et al.[22] $E_0 = 66.4 \pm 3.0$ kJ mol^{-1} is obtained, which is in agreement with the value $E_0 = \Delta_r H^0_0 = 68.0 \pm 2.8$ kJ mol^{-1} derived by Plenge et al.[14] from their photoionization data for ClO and ClOOCl.

C. Temperature Dependence of $K_{eq} = k_1/k_{-1}$. Literature values of K_{eq} vary by a factor of about 2 at 298 K and a factor of about 3 at 250 K (Table 4). The equilibrium has been studied between 233 and 310 K in the laboratory and (due to the lower concentrations) between 188 and 216 K in the nighttime polar stratosphere. The values of the dissociation rate constants k_{-1} measured in this work and the corresponding low-pressure recombination rate constants k_1 from the literature may be used to determine equilibrium constants K_{eq} via

$$K_{eq} = k_1/k_{-1} \quad \text{(III)}$$

Equilibrium constants K_p are calculated from the individual data points of k_{-1} summarized in Table 2 and the k_1 values recommended in ref 6. A least-squares fit of a K_p(T) plot according to

$$\ln K_p = A + B/T \quad \text{(IV)}$$

is shown in Figure 9. The data points (open and full squares) are represented by the expression (full straight line):

$$\ln(K_p/\mathrm{atm}^{-1}) = -(20.4 \pm 3.2) + (9422 \pm 800)\,\mathrm{K}/T \quad (2\sigma) \quad \text{(V)}$$

From eq V, $\Delta_r H^0_{251K}$ (ClOOCl ⇒ 2ClO) = 78.3 ± 6.7 kJ mol^{-1} (2s) is derived, which is slightly larger than the range of values present in the literature (69−76 kJ mol^{-1}; see Table 4). In Figure 9, the present results are compared with data from Cox and Hayman[26] and Plenge et al.[14] The K_p values recommended in the most recent JPL data compilation[6] are based on the data of Cox and Hayman[26] and Nickolaisen et al.[20] and are also included in Figure 9.

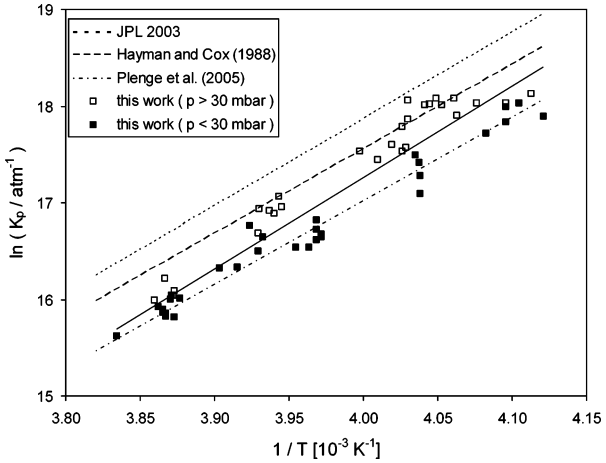

Figure 9. Equilibrium constants k_1/k_{-1} from laboratory studies: full straight line, least-squares fit to the complete data set from this work; full and open squares, k_{-1} from Table 2 combined with k_1 from the most recent JPL evaluation.[6]

The data points in Figure 9 are strongly scattered. However, the scatter is mainly due to a pressure dependence of the calculated values of K_p. Because K_p must be independent of pressure, this result means that either the recombination data from ref 6 or the dissociation data from the present work or

both are subject to a pressure dependent error. This becomes evident when the data points are subdivided into two groups, those at "low pressures" ($p_{tot} < 30$ mbar) and those at "high pressures" ($p_{tot} > 30$ mbar) (full and open squares). Because the reason for this pressure dependence is yet unknown, the least-squares fit to the complete data set is shown by the full straight line. There are several conclusions that can be drawn from Figure 9:

(i) All the equilibrium constants k_1/k_{-1} derived from this work (k_{-1}) and ref 6 (k_1) are below the values recommended in the most recent JPL evaluation[6] by an average factor of 1.8.

(ii) The scatter of the data is lowest for high temperatures; at these conditions the values are lower than the recommended values by a factor of about 2.

(iii) The scatter of the equilibrium constants is considerably lower for the "low pressure" values than for the "high pressure" values or the complete data set ($\Delta B = \pm 530$ K as compared to ± 930 K and ± 800 K, respectively; 2σ). In addition, the slope of the least squares line through the "low pressure" data is similar to the slopes of the fits to the data of Cox and Hayman,[26] Plenge et al.[14] and JPL[6] whereas the slopes through the high pressure data and the complete data set are considerably larger. Thus the data at low pressures, represented by

$$K_c = 8.0 \times 10^{-27} \exp[(8073 \pm 530)\ \mathrm{K}/T] \qquad (2\sigma) \quad \text{(VI)}$$

are considered to be more reliable and are included in Table 4 as the results of this work.

Recently, laboratory data on the ClO/ClOOCl reaction system were discussed related to the interpretation of mixing ratios of ClO and ClOOCl measured in the polar stratosphere at night. The nighttime ClO concentrations are controlled by thermal equilibrium between ClO and ClOOCl, and the formation rates of ClO measured in the early morning are sensitive to the nighttime equilibrium concentrations of ClO. The field measurements generally favor higher concentrations of ClO at night than is inferred from recommended[6] equilibrium constants k_1/k_{-1}. Discussion of the field data in the work of Plenge et al.[14] shows that the equilibrium data from the present work lie between the data inferred from the field measurements of Vogel et al.[8] and von Hobe et al.,[10] and fit very well to the concentrations measured by Avallone and Toohey[7] and Stimpfle et al.[5] in the Arctic polar stratosphere.

With respect to the laboratory data, the present K_p values lie between the data of Cox and Hayman[26] and of Plenge et al.[14] (Note: the line representing the results of Plenge et al.[14] resembles a least-squares fit to the subset of our low-pressure data (full squares)).

Until recently, the high-temperature laboratory data on K_{eq} could not reliably be extrapolated to the temperatures of the polar stratosphere, i.e., 190−210 K. The K_{eq} values deduced from the ClO and ClOOCl measurements in the polar stratosphere are also subject to systematic errors due to the special difficulties inherent in field measurements in this particular environment. The situation has improved due to results of Plenge et al.[14] providing a new accurate value for the dissociation energy of ClOOCl. Because the error of their $\Delta_r H^0$ value (stated error: ± 2.8 kJ mol^{-1}) results in an error of about a factor of 4 for K_{eq}, the safest way to fix K_{eq} over a large temperature regime may still be the combination of absolute values from field measurements at around 200 K and from laboratory work close to room temperature.

The most complete data set on K_{eq} around 200 K seems to be that of Avallone and Toohey[7] who measured ClO in the Arctic stratosphere during winter and assumed [ClOOCl] to be $^1/_2$([total inorganic chlorine] − [ClO]). Both [ClO] and [ClOOCl] were simultaneously measured by Stimpfle et al.[5] and von Hobe et al.[10] Whereas Stimpfle et al. state that their data are well reproduced using the van't Hoff expression of Cox and Hayman and the equilibrium constants of Avallone and Toohey, von Hobe et al. find values that are lower by more than a factor of 3. A weighted average of the results of these three field studies leads us to $K_{eq} = 6.1 \times 10^{-9}$ cm^3 molecule^{-1} at 200 K. In the high-temperature regime, the most accurate value of K_{eq} can be obtained from laboratory investigations around room temperature. From the experimental results of Basco and Hunt,[16] Cox and Hayman,[26] Nickolaisen et al.,[20] Horowitz et al.,[27] Ellermann et al.,[21] Plenge et al.,[14] and the present work, we estimate a weighted mean value of $K_{eq} = 5.8 \times 10^{-15}$ cm^3 molecule^{-1} at 298 K. We feel that the present accuracy of the data on K_{eq} does not justify the use of expressions more complex than eq IV for the temperature dependence of K_{eq}. The combination of the above K_{eq} values at 200 and 298 K results in

$$K_c = A \times \exp(B/T) = 3.0 \times 10^{-27} \exp(8433\ \mathrm{K}/T)\ \mathrm{cm}^3\ \mathrm{molecule}^{-1} \quad \text{(VII)}$$

Equation VII fits well to the following data:

(i) Necessarily, it fits to the main body of laboratory data at and slightly below room temperature and at the temperatures of the polar stratosphere because parameters A and B in eq VII are based on these data.

(ii) At 250 K, eq VII gives $K_c = 1.34 \times 10^{-12}$ cm^3 molecule^{-1}, which agrees with our value of the runs for $p > 30$ mbar and is still close to our data for $p < 30$ mbar.

(iii) $B = 8433$ K from eq VII corresponds to $\Delta_r H^0_{239} = 72.1$ kJ mol^{-1}. This value is in perfect agreement with $\Delta_r H^0_{298} = 72.4 \pm 2.8$ kJ mol^{-1} derived by Plenge et al.[14] from their photoionization study and with the value $\Delta_r H^0_{263} = 72.5 \pm 3$ kJ mol^{-1} from the equilibrium study of Cox and Hayman[26] at 1 atm (where the influence of the bimolecular channels 4a−4c is strongly reduced in favor of the pressure dependent recombination channel).

Summary

The thermal decomposition of ClOOCl, which is of considerable interest for the stratospheric ozone loss, has been investigated in a moderate temperature range and a large range of total pressures. Depending on temperature and pressure, the decomposition rate constants differ from a study of Nickolaisen et al.[20] by factors between 1.5 and 4.2. The reason for this discrepancy is yet unknown. Combination of the present dissociation data with the recommended[6] rate constants for the reverse reaction from the literature leads to pressure dependent equilibrium constants, thus demonstrating inconsistencies between the dissociation and recombination data. These equilibrium constants support evidence from field measurements of ClO and ClOOCl in the polar stratosphere that the presently recommended equilibrium constants of the ClO + ClO ⇔ ClOOCl equilibrium[6] are too high and lead to lower ClO concentrations in the nighttime polar stratosphere than are observed. In addition, recent results including the present work suggest a ClO−OCl bond energy that is lower than the currently recommended value by about 3 kJ mol^{-1}. $K_c = 3.0 \times 10^{-27}$ exp(8433 K/T) cm^{3}molecule^{-1} is recommended for the temperature dependence of K_{eq}, which fits most of the data at low and high temperatures.

Acknowledgment. Financial support of this work by the EU under contract no. EV5V-CT93-0338 is gratefully acknowledged.

References and Notes

(1) Molina, L. T.; Molina, M. J. *J. Phys. Chem.* **1987**, *91*, 433.
(2) Solomon, S. *Rev. Geophys.* **1988**, *26*, 131.
(3) Anderson, J. G.; Brune, W. H.; Lloyd, S. A.; Toohey, D. W. *J. Geophys. Res.* **1989**, *94*, 11480.
(4) Brune, W. H.; Anderson, J. G.; Toohey, D. W.; Fahey, D. W.; Kawa, S. R.; Jones, R. L.; McKenna, D. S.; Poole, L. R. *Science* **1991**, *252*, 1260.
(5) Stimpfle, R. M.; Wilmouth, D. M.; Salawitch, R. J.; Anderson, J. G. *J. Geophys. Res.* **2004**, *109* (*D3*), D03301, DOI: 10.1029/2003JD003811.
(6) Sander, S. P.; Friedl, R. R.; Golden, D. M.; Kurylo, M. J.; Huie, R. E.; Orkin, V. L.; Moortgat, G. K.; Ravishankara, A. R.; Kolb, C. E.; Molina, M. J.; Finlayson-Pitts, B. J. *Chemical Kinetics and Photochemical Data for Use in Atmospheric Studies*; Evaluation No. 14; Jet Propulsion Laboratory: Pasadena, CA, 2003.
(7) Avallone, L. M.; Toohey, D. W. *J. Geophys. Res.* **2001**, *106*, 10411.
(8) Vogel, B.; Stroh, F.; Grooss, J.-U.; Müller, R.; Deshler, T.; Karhu, J.; McKenna, D. S.; Müller, M.; Toohey, D.; Toon, G. *J. Geophys. Res.* **2003**, *108*, 8334; DOI: 10.1029/2002JD002564.
(9) Vogel, B.; Müller, R.; Engel, A.; Grooss, J.-U.; Toohey, D.; Woyke, T.; Stroh, F. *Atmos. Chem. Phys.* **2005**, *5*, 1623.
(10) von Hobe, M.; Grooss, J.-U.; Müller, R.; Hrechanyy, S.; Winkler, U.; Stroh, F. *Atmos. Chem. Phys.* **2005**, *5*, 693.
(11) Shindell, D. T.; deZafra, R. L. *Geophys. Res. Lett.* **1995**, *22*, 3215.
(12) Rex, M.; Salawitch, R. J.; Santee, M. L.; Waters, J. W.; Hoppel, K.; Bevilacqua, R. *Geophys. Res. Lett.* **2003**, *30* (1), 1008; DOI: 10.1029/2002GL016008.
(13) Pierson, J. M.; McKinney, K. A.; Toohey, D. W.; Margitan, J.; Schmidt, U.; Engel, A.; Newman, P. A. *J. Atmos. Chem.* **1999**, *32*, 61.
(14) Plenge, J.; Kühl, S.; Vogel, B.; Müller, R.; Stroh, F.; von Hobe, M.; Flesch, R.; Rühl, E. *J. Phys. Chem. A* **2005**, *109*, 6730.
(15) Johnston, H. S.; Morris, E. D., Jr.; van den Bogaerde, J. *J. Am. Chem. Soc.* **1969**, *91*, 7712.
(16) Basco, N.; Hunt, J. E. *Int. J. Chem. Kinet.* **1979**, *11*, 649.
(17) Hayman, G. D.;. Davies, M.; Cox, R. A. *Geophys. Res. Lett.* **1986**, *13*, 1347.
(18) Sander, S. P.; Friedl, R. P.; Yung, Y. L. *Science* **1989**, *245*, 1095.
(19) Trolier, M.; Mauldin, R. L., III; Ravishankara, A. R. *J. Phys. Chem.* **1990**, *94*, 4896.
(20) Nickolaisen, S. L.; Friedl, R. R.; Sander, S. P. *J. Phys. Chem.* **1994**, *98*, 155.
(21) Ellermann, T.; Johnsson, K.; Lund, A.; Pagsberg, P. *Acta Chim. Scand.* **1995**, *49*, 28.
(22) Bloss, W. J.; Nickolaisen, S. L.; Salawitch, R. J.; Friedl, R. R.; Sander, S. P. *J. Phys. Chem. A* **2001**, *105*, 11226.
(23) Zhu, R. S.; Lin, M. C. *J. Chem. Phys.* **2003**, *118*, 4094.
(24) Atkinson, R.; Baulch, D. L.; Cox, R. A.; Hampson, R. F., Jr.; Kerr, J. A.; Rossi, M.; Troe, J. *J. Phys. Chem. Ref. Data* **1999**, *28*, 191.
(25) Wayne, R. P.; Poulet, G.; Biggs, P.; Burrows, J. P.; Cox, R. A.; Crutzen, P. J.; Hayman, G. D.; Jenkin, M. E.; Le Bras, G.; Moortgart, G. K.; Platt, U.; Schindler, R. N. *Atmos. Environ.* **1995**, *29*, 2675.
(26) Cox, R. A.; Hayman, G. D. *Nature* **1988**, *332*, 796.
(27) Horowitz, A.; Crowley, J. N.; Moortgat, G. K. *J. Phys. Chem.* **1994**, *98*, 11924.
(28) Cox, R. A.; Derwent, R. G. *J. Chem. Soc., Faraday Trans. 1* **1979**, *75*, 1635.
(29) A major part of the present data have been presented at the 13th International Symposium on Gas Kinetics, 11−16th September, 1994, Dublin; Abstract Book, abstract no. D45, p 336.
(30) Barnes, I.; Becker, K. H.; Fink, E. H.; Reimer, A.; Zabel, F.; Niki, H. *Int. J. Chem. Kinet.* **1983**, *15*, 631.
(31) Zabel, F. *Ber. Bunsen-Ges. Phys. Chem.* **1991**, *95*, 893.
(32) Birk, M.; Friedl, R. R.; Cohen, E. A.; Pickett H. M.; Sander, S. P. *J. Chem. Phys.* **1989**, *91*, 6588.
(33) McGrath, M. P.; Clemitshaw, K. C.; Rowland, F. S.; Hehre, W. J. *Geophys. Res. Lett.* **1988**, *15*, 883.
(34) Stanton, J. F.; Rittby, C. M.; Bartlett, R. J.; Toohey, D. W. *J. Phys. Chem.* **1991**, *95*, 2107.
(35) Lee, T. J.; Rohlfing, C. M.; Rice, J. E. *J. Chem. Phys.* **1992**, *97*, 6593.
(36) Müller, H. S. P.; Willner, H. *Ber. Bunsen-Ges. Phys. Chem.* **1992**, *96*, 427.
(37) Graham, J. D.; Roberts, J. T.; Anderson, L. D.; Grassian, V. H. *J. Phys. Chem.* **1996**, *100*, 19551.
(38) McKeachie, J. R.; Appel, M. F.; Kirchner, U.; Schindler, R. N.; Benter, Th. *J. Phys. Chem. B* **2004**, *108*, 16786.
(39) Anderson, L. C.; Fahey, D. W. *J. Phys. Chem.* **1990**, *94*, 644.
(40) Deuflhard, P.; Nowak, U. *Ber. Bunsen-Ges. Phys. Chem.* **1986**, *90*, 940.
(41) Brauer, H. *Handbuch der Präparativen Chemie*; Springer: Heidelberg, 1979.
(42) Burkholder, J. B.; Orlando, J. J.; Howard, C. J. *J. Phys. Chem.* **1990**, *94*, 687.
(43) Brust, A.; Zabel, F.; Becker K. H. *Geophys. Res. Lett.* **1997**, *24*, 1395.
(44) Lopez, M. I.; Sicre, J. E. *J. Phys. Chem.* **1988**, *92*, 563.
(45) Molina, L. T.; Molina, M. J. *J. Photochem.* **1979**, *11*, 139.
(46) Chang, Y. S.; Shaw, J. H.; Niple, E.; Calvert, J. G.; Chan, W. H.; Levine, S. Z.; Uselman, W. M. Application of Fourier Transform Spectroscopy to Air Pollution Problems; EPA Interim Report; EPA: Washington, DC, 1977.
(47) Illies, A. J.; Takacs, G. A. *J. Photochem.* **1976**, *6*, 35.
(48) Burkholder, J. B.; Talukdar, R. K.; Ravishankara, A. R.; Solomon, S. *J. Geophys. Res.* **1993**, *98*, 22937.
(49) Christe, K. O.; Schack, C. J.; Curtis, E. C. *Inorg. Chem.* **1971**, *10*, 1589.
(50) Tuazon, E. C.; Wallington, T. J. *Geophys. Res. Lett.* **1989**, *16*, 331.
(51) Parr, A. D.; Wayne, R. P.; Hayman, G. D.; Jenkin, M. E.; Cox, R. A. *Geophys. Res. Lett.* **1990**, *17*, 2357.
(52) Burkholder, J. B.; Mauldin, R. L., III; Yokelson, R. J.; Solomon, S.; Ravishankara, A. R. *J. Phys. Chem.* **1993**, *97*, 7597.
(53) Hayman, G. D.; Cox, R. A. *Chem. Phys. Lett.* **1989**, *155*, 1.
(54) Troe, J. *J. Phys. Chem.* **1979**, *83*, 114.
(55) DeMore, W. B.; Tschuikow-Roux, E. *J. Phys. Chem.* **1990**, *94*, 5856.
(56) Bröske, R.; Zabel, F. Data presented at the Third European Symposium on Polar Stratospheric Ozone, 18−22 September, 1995, Schliersee (Bavaria, Germany).
(57) Note: The experimental heat of formation of ClOOCl at 0 K from Nickolaisen et al.[20] cited in ref 23 (Table 2 and text) is from Second Law analysis. Nickolaisen et al. state that they prefer their Third Law result, which is larger by 1.6 kcal mol^{-1}. Then the average of the two experimental values is 31.9 kcal mol^{-1} as compared to the ab initio value of 29.4 kcal mol^{-1} from Zhu and Lin.[23]
(58) Troe, J. *J. Chem. Phys.* **1977**, *66*, 4758.
(59) Zabel, F. Habilitation Thesis, Wuppertal, 1992.
(60) Jacobs, J.; Kronberg, M.; Müller, H. S. P.; Willner, H. *J. Am. Chem. Soc.* **1994**, *116*, 1106.